INTERNATIONAL JOURNAL OF INTELLIGENT CONTROL AND SYSTEMS
VOL.15,NO.1,MARCH 2010,18-24

Active Disturbance Rejection Control for an Electric Power Assist Steering System

Lili DONG[1, *], *Member, IEEE,* Prasanth KANDULA[1], Zhiqiang GAO[1], *Member, IEEE,* Dexin WANG[2]

Abstract—**This paper presents the application of an active disturbance rejection controller (ADRC) to an electrical power assist steering system (EPAS) in automobiles. The control objective is to reduce the steering torque exerted by a driver so as to achieve good steering feel in the presence of external disturbances and system uncertainties. With the proposed ADRC, the driver can turn the steering wheel with the desired steering torque which is independent of load torques that tend to vary depending on driving conditions. The ADRC is constructed on a column-type EPAS model. The computer simulation and frequency-domain analyses verify the robustness and stability of the ADRC controlled system.**

***Index Terms*—EPAS, active disturbance rejection control, robustness, system uncertainty, external disturbance, automobile.**

I. INTRODUCTION

A steering system is one of major subsystems for vehicle operation [1]. The most conventional steering arrangement is to turn the front wheel using a hand–operated steering wheel which is positioned in front of the driver, via the steering column. However, as vehicles have become heavier and switched to front wheel drive, the effort to turn the steering wheel manually will be greatly increased, often to the point where major physical exertion is required. To alleviate this, automobile manufacturers have developed power steering systems. In modern world, there are two major types of power steering systems: hydraulic and electric. A hydraulic power steering (HPS) system uses hydraulic pressure supplied by an engine-driven pump to assist the motion of turning the steering wheel. Electric power assist steering (EPAS) is more efficient than the hydraulic power steering, since the electric power steering motor only needs to provide assistance when the steering wheel is turned, whereas the hydraulic pump must run constantly. In addition, the EPAS system has the advantages of fuel economy, space efficiency, and environmental protection [2, 3] over the HPS system. The EPAS system has begun replacing the HPS system in some advanced small vehicles. The utilization of the EPAS to all types of vehicles is expected to be expanded exponentially [4] in the future.

The essence of an EPAS system is an electronically controlled assist motor [5] that can be taken as a smart actuator. The EPAS is a classical example of the actuator operating under feedback control [6]. When an appropriate assist torque from the assist motor is applied in the same direction as the driver's steering direction, the amount of steering torque required by the driver for steering can be considerably relieved. Therefore the controller in EPAS aims at driving the motor to output the assist torque so as to improve the steering feel of the driver. The high performance requirements of the EPAS in automobile industry also require the control system to be robust against modeling uncertainties and unknown disturbances. Specifically, a controller is crucial for the EPAS system to stabilize the feedback system with torque sensor and actuator (motor), to reduce the steering torque, and to improve the steering feel of the driver.

There has been much research and development performed on EPAS systems though detailed information on their control strategies has not been extensively released in the literature [7]. Most of the current research [1-6] has successfully employed high-order lead-lag compensator or Proportional Integral Derivative (PID) controller to reach the control objective given above. However, the multiple tuning parameters of the compensator (with 4 or 5 tuning parameters) and PID controller (with at least 3 tuning parameters) make them difficult to adjust and implement in the real world. In addition, the compensator and PID controller are sensitive to both unknown external disturbances and parameter variations. Their performances are greatly degraded in the presence of the disturbance and structural uncertainties that are common in the EPAS system. Hence dealing with the uncertain dynamics in EPAS systems makes the control problem extremely challenging and critically important. A limited amount of research is reported using the advanced controller such as H_2-norm or H^∞ approach [8, 9] to solve the robustness problem. But the implementations of such advanced controllers in practice are also restricted by their complex configurations and multiple tuning parameters. Therefore, finding a simple-to-implement control solution being robust against uncertainties and disturbances will have wide impacts on the deployment of the EPAS in the next generation of vehicles.

The paper presents the employment of an emerging practical control strategy that is Active Disturbance Rejection Control (ADRC) [10-14] to the EPAS system. The controller treats the discrepancy between the real EPAS system and its mathematical model as the generalized disturbance and actively estimates and rejects the disturbance in real time,

[1]The authors are with the Department of Electrical & Computer Engineering, Cleveland State University, Cleveland, OH 44115 USA.
[2]The author is with Ford Motor Corp., Dearborn, MI 48121, USA.
*Corresponding author. Email: L.Dong34@csuohio.edu.

hence the name ADRC. Since the controller design is not based on the accurate mathematical model of a system, it is very effective in dealing with a large amount of uncertainties and external disturbances, the main challenges pertaining to EPAS systems. For the first time, we modify the controller and extend its use to the EPAS systems.

The rest of this paper is organized as follows. The dynamic modeling of an EPAS system is given in section II. The design of ADRC is presented in section III. The stability and robust analyses are included in section IV. The simulation results are shown in section V. Section VI gives concluding remarks and suggests future research.

II. Dynamic Model of an EPAS System

We choose a column-type EPAS system to design its controller. The plant includes the steering wheel-column-torque sensor assembly, the steering rack shaft, and the electric motor-gear box assembly. The mechanical model is extracted from [1] and shown in Fig.1, where T_s denotes steering torque, T_m motor torque, T_a the assist torque delivered to the shaft, T_l load torque, θ_m motor angle, θ_{ss} the angular position at the steering shaft, and θ_{sw} the angular position at the steering wheel.

A major function of the EPAS system is reduction in steering torque for improving the steering feel of the driver. In order to realize the function, a proper amount of assist torque should be provided by the assist motor to reduce the driver's steering torque. So a steer controller is applied to drive the assist motor to output the assist torque. A block diagram of the EPAS control system is shown in Fig. 2, in which T_{rs} is a reference steering torque, F_d is an external disturbance, and u is the control input to the assist motor. The reference torque is also taken as the desired assist torque. It can be determined based on the information of vehicle speed and steering wheel angle θ_{sw} [1].

In Fig.2, the dynamics of the sensor and the motor can be modeled as

$$P(s)=\frac{P_t}{s+P_t}\frac{P_a}{s+P_a}, \tag{1}$$

where $-P_t$ and $-P_a$ are the poles of torque sensor and actuator. The transfer function of steering column and rack system is represented by

$$G(s)=\frac{K_S}{R_S^2}\frac{J_S s^2+b_S s}{(J_S s^2+b_S s+K_S)(m_e s^2+b_e s+K_e)}, \tag{2}$$

where m_e and b_e are effective rack mass and damping coefficient; J_s, b_s, and K_s are moment of inertia, damping coefficient and stiffness of the steering column. The parameters values in (1) and (2) are listed in Table II in Appendix. From (1) and (2), the transfer function representation of the block diagram in Fig. 2 can be illustrated as Fig. 3, where *P(s)* represents the dynamics of the sensor and the actuator (motor), K_a is a feed-forward gain from the actuator, *G(s)* is the transfer function of the steering column and rack system, T_s is a measured steering torque, and *C(s)* represents the controller to be designed.

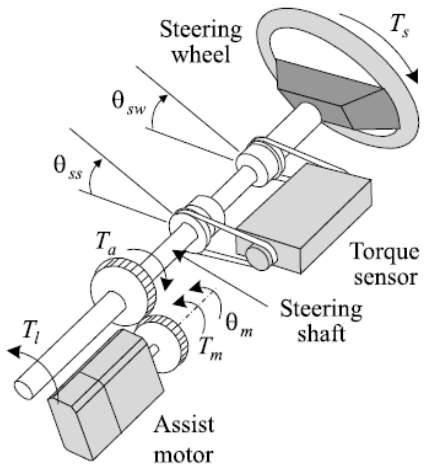

Fig.1: The dynamic model of an EPAS system [1]

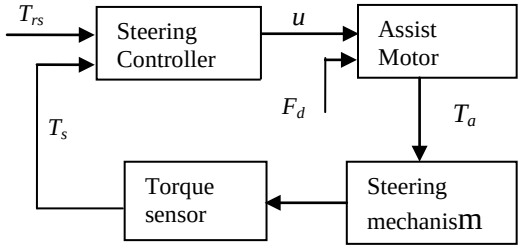

Fig. 2: Block diagram of the steering control system

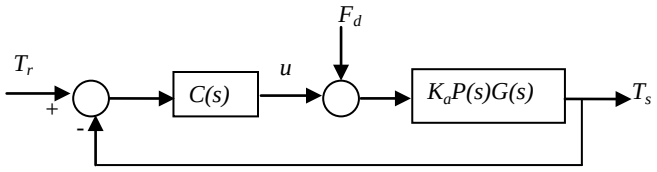

Fig. 3: Transfer function representation of EPAS control system

III. Controller Design

Define $y=T_s$. The open-loop transfer function of the plant in Fig. 3 can be represented by

$$\frac{y(s)}{u(s)+F_d(s)}=K_aP(s)G(s)$$
$$=\frac{K_aK_s}{R_s^2}\frac{p_tp_a(J_s s^2+b_s s)}{(s+P_t)(s+P_a)(J_s s^2+b_s s+K_s)(m_e s^2+b_e s+K_e)} \tag{3}$$

Since the product of *P(s)* and *G(s)* is a sixth-order system, the transfer function (3) can be rewritten as

$$\frac{y(s)}{u(s)+F_d(s)}=\frac{a_2 s^2+a_1 s}{b_6 s^6+b_5 s^5+b_4 s^4+b_3 s^3+b_2 s^2+b_1 s+b_0} \tag{4}$$

where the parameters a_i and b_i are the coefficients of the numerator and denominator of the transfer function (4). The coefficients can be obtained through comparing the right sides of equations (3) and (4). Converting the transfer function (4) to an ODE form yields

$$b_6y^{(6)}+b_5y^{(5)}+b_4y^{(4)}+b_3y^{(3)}+b_2y''+b_1y'+b_0y=a_2u''+a_1u'$$
$$+a_1F_d''+a_1F_d'. \tag{5}$$

Integrating both sides of (5) double times, we will have

$$y^{(4)} = f(y^{(3)}, y'', y', y, \int y, \iint y, \int u, F_d, \int F_d) + \frac{a_2}{b_6} u \tag{6}$$

where $f(y^{(3)}, y'', y', y, \int y, \iint y, \int u, F_d, \int F_d)$, also denoted as *f*, is taken as a generalized disturbance including internal dynamics and unknown external disturbances. The basic idea of the ADRC is to estimate the generalized disturbance using an Extended State Observer (ESO), and actively cancel it in real time to reduce the original system model (6) to a multiple integrator. Then a traditional proportional derivative controller will be used to drive the measured torque output *y* to a desired value. Following the analysis above, we rewrite (6) as:

$$y^{(4)} = f + \beta u, \tag{7}$$

where $\beta = a_2/b_6$ is a controller gain. We suppose $\hat{f}$ is an estimated *f* through the ESO. Then the controller:

$$u = \frac{1}{\beta}(-\hat{f} + u_0), \tag{8}$$

reduces (7) to a merely multiple integral plant of the form

$$y^{(4)} = f - \hat{f} + u_0 \approx u_0, \tag{9}$$

which can be readily driven to the desired torque by a proportional derivative (PD) controller. Let *r* denote the reference torque and $r = T_{rs}$. So the tracking error $e = r - y$. Then the PD controller can be represented by

$$u_0 = k_p e - k_{d1}\dot{e} - k_{d2}\ddot{e} - k_{d3}\dddot{e}, \tag{10}$$

where the controller gains are selected as

$$k_{di} = C_4^i \omega_c^{4-i}, i = 0,1,2,3. \tag{11}$$

In this way, the only tuning parameter of the controller is the controller bandwidth ω_c and all the closed-loop poles are set to $-\omega_c$. As analyzed above, the performance of the ADRC is rigorously dependent on the accurate estimation of the ESO whose design is stated as follows.

We suppose function *f* is continuous and its derivative is bounded. Then the ESO including one augmented state *f* can be represented by

$$\begin{aligned} \dot{z} &= Az + Bu + L(y - \hat{y}), \\ \hat{y} &= Cz \end{aligned} \tag{12}$$

where $A = \begin{bmatrix} 1 & 0 & 0 & 0 & 0 \\ 0 & 1 & 0 & 0 & 0 \\ 0 & 0 & 1 & 0 & 0 \\ 0 & 0 & 0 & 1 & 0 \\ 0 & 0 & 0 & 0 & 0 \end{bmatrix}, B = \begin{bmatrix} 0 \\ 0 \\ 0 \\ \beta \\ 0 \end{bmatrix}, C = [1 \quad 0 \quad 0 \quad 0 \quad 0], z = \begin{bmatrix} \hat{y} \\ \dot{\hat{y}} \\ \ddot{\hat{y}} \\ \dddot{\hat{y}} \\ \hat{f} \end{bmatrix}$,

$L = \begin{bmatrix} 5\omega_o & 10\omega_o^2 & 10\omega_o^3 & 5\omega_o^4 & \omega_o^5 \end{bmatrix} = \begin{bmatrix} l_1 & l_2 & l_3 & l_4 & l_5 \end{bmatrix}$, and *z* is the estimated state vector, in which $\hat{y}$ is the estimated *y*, $\dot{\hat{y}}$ the estimated $\dot{y}$, $\ddot{\hat{y}}$ the estimated $\ddot{y}$, and $\dddot{\hat{y}}$ the estimated $\dddot{y}$. The vector *L* is denoted as observer gain vector and ω_o is observer bandwidth. Similarly, the observer gains of the ESO have been chosen such that all the eigenvalues of the ESO equal - ω_o. From (11) and (12), we can see that in order to reach the control objective, only two tuning parameters are needed for the ADRC. They are the bandwidths (ω_o and ω_c) of the controller and observer respectively. The details about how to tune the parameters of the ADRC are explained in [16]. For tuning simplicity, we generally choose $\omega_o = 5\omega_c$ [16]. So eventually there is just one tuning parameter, which is ω_c, for the ADRC controller.

In summary, the proposed ADRC design proves to be a good fit for an EPAS system for three reasons: 1) it requires minimal a priori information of the plant (just the relative order of the plant and its highest-order gain [11]), 2) it actively estimates and compensates the unknown dynamics and disturbances, 3) the controller only has one tuning parameter, which is easy to be implemented and tuned, compared to other methods.

IV. PERFORMANCE AND ROBUSTNESS ANALYSES

In this section, the steady-state performance of the closed-loop control system is discussed. In addition, the robustness of ADRC against parameter variations is analyzed through frequency responses. The frequency-domain analyses of ADRC are initially reported in [16]. This paper originally employed the frequency-domain analyses to the EPAS system.

A. Transfer function expression of an EPAS control system

The Lapalce transform of the ESO given by (12) is

$$sZ(s) = (A - LC)Z(s) + LY(s) + BU(s), \tag{13}$$

where *Z(s)* is the Laplace transform of the estimated state vector. The Laplace transform of the controller represented by (8) and (10) is

$$U(s) = \frac{1}{\beta}\begin{bmatrix} k_p & k_{d1} & k_{d2} & k_{d3} \end{bmatrix}\begin{bmatrix} R(s) \\ sR(s) \\ s^2R(s) \\ s^3R(s) \end{bmatrix} - \frac{1}{\beta}\begin{bmatrix} k_p & k_{d1} & k_{d2} & k_{d3} & 1 \end{bmatrix}Z(s) \tag{14}$$

Substituting (14) into (13) yields

$$U(s) = H(s)G_c(s)R(s) - G_c(s)Z(s). \tag{15}$$

In (15),

$$H(s) = \frac{(s^5 + l_1 s^4 + l_2 s^3 + l_3 s^2 + l_4 s + l_5)(k_p + k_{d1}s + k_{d2}s^2 + k_{d3}s^3 + s^4)}{\mu_1 s^4 + \mu_2 s^3 + \mu_3 s^2 + \mu_4 s + \mu_5}, \tag{16}$$

where $\mu_1 = l_1 k_p + l_2 k_{d1} + l_3 k_{d2} + l_4 k_{d3} + l_5$, $\mu_2 = l_2 k_p + l_3 k_{d1} + k_4 k_{d2} + l_5 k_{d3}$, $\mu_3 = l_3 k_p + l_4 k_{d1} + l_5 k_{d2}$, $\mu_4 = l_4 k_p + l_5 k_{d1}$, $\mu_5 = l_5 k_p$, and

$$G_c(s) = \frac{\mu_1 s^4 + \mu_2 s^3 + \mu_3 s^2 + \mu_4 s + \mu_5}{\beta(s^5 + \lambda_1 s^4 + \lambda_2 s^3 + \lambda_3 s^2 + \lambda_4 s)}, \tag{17}$$

where $\lambda_1 = k_{d3} + l_1$, $\lambda_2 = k_{d2} + k_{d3}l_1 + l_2$, $\lambda_3 = k_{d1} + k_{d2}l_1 + k_{d3}l_2 + l_3$, and $\lambda_4 = k_p + k_{d1}l_1 + k_{d2}l_2 + k_{d3}l_3 + l_4$.

According to (15), (16) and (17), the block diagram of the closed-loop control system can be represented by Fig. 4, where the plant $G_p(s)$ is equal to $K_a P(s) G(s)$ as given in (3).

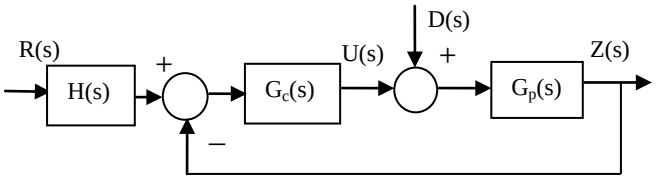

Fig.4: Block diagram of the closed-loop control system

From Fig.4, the open-loop transfer function is

$$G_o(s) = G_c(s)G_p(s)\cdot \tag{18}$$

The closed-loop transfer function is

$$G_{cl}(s) = \frac{Z(s)}{R(s)} = \frac{H(s)G_c(s)G_p(s)}{1+G_c(s)G_p(s)}\ . \tag{19}$$

In addition, the transfer function from the disturbance input to the torque output is

$$G_d(s) = \frac{Z(s)}{D(s)} = \frac{G_p(s)}{1+G_c(s)G_p(s)}\ . \tag{20}$$

B. *Convergence of tracking error*

In Fig. 4, the reference signal *R(s)* (or desired assist steering torque) for the EPAS system is usually a sinusoidal signal [8] and its expression is $R(s)=A\sin(\omega t)$. According to (19), the steady-state output of the EPAS system is

$$x_{ss} = A\left|G_{cl}(j\omega)\right|\sin(\omega t+\phi), \tag{21}$$

where the phase shift is

$$\phi = \angle G_{cl}(j\omega) = \tan^{-1}\frac{\mathrm{Im}(G_{cl}(j\omega))}{\mathrm{Re}(G_{cl}(j\omega))}. \tag{22}$$

Define the magnitude error between the steady-state output of the EPAS and the reference signal as $e_m=A-A|G_{cl}(j\omega)|$. The e_m and Φ versus the controller gain ω_c are shown in Fig. 5, where both the magnitude error and the phase shift of the stead-state output of the EPAS system are converging to zeros with the increase of the controller bandwidth ω_c. According to Fig. 5, we choose $\omega_c=5\times10^3$ *rad/s*, for which e_m is about 0.6% of the reference magnitude and $\Phi=-6\times10^{-5}$*rad*, in the following computer simulations of the ADRC.

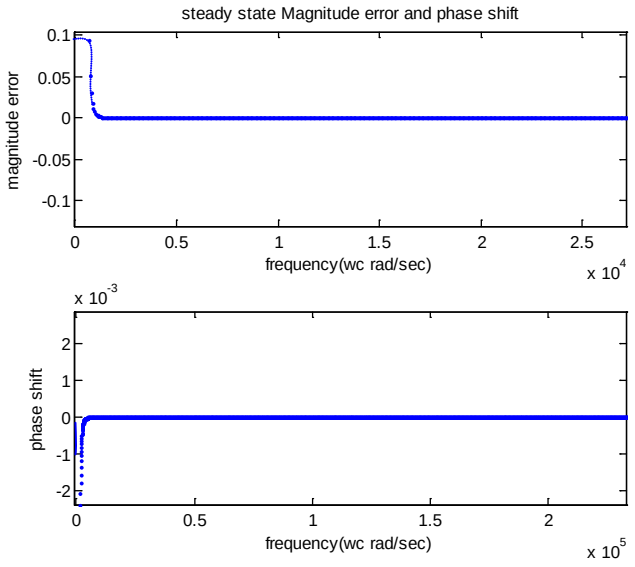

Fig.5: The steady-state magnitude error and phase shift

C. *External disturbance rejection*

This section will show how the external disturbance is rejected by the ADRC in the presence of structural uncertainties of the EPAS system. Substituting $G_p(s)$ in (3) and $G_c(s)$ in (17) into (20), we have

$$G_d(s) = \frac{\beta s(a_2s^5+(a_2\lambda_1+a_1)s^4+(a_2\lambda_2+a_1\lambda_1)s^3+(a_1\lambda_2+a_2\lambda_3)s^2+(a_2\lambda_4+a_1\lambda_3)s+a_1\lambda_4)}{A_d(s)}, \tag{23}$$

where $A_d(s)$, given in Appendix, is a tenth-order polynomial including non-zero constant term. From (23), we can see that as the input frequency ω goes to zero or infinite, $G_d(j\omega)$ will converge to zero. This suggests that the disturbance will be attenuated to zero with the increase of system bandwidth. The Bode plots of (23) are shown in Fig. 6, in which the system parameters (J_s, b_s, K_s, R_s, m, J_m, R_m, b_m and b) are varying from the nominal values listed in Table II in Appendix to 20% of their nominal values. The figure demonstrated a desirable disturbance rejection property in the presence of the variations of the system parameters.

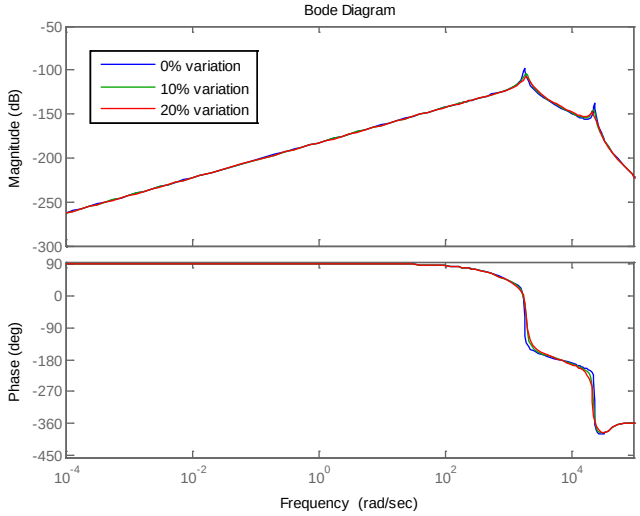

Fig.6: the Bode diagrams of $G_d(s)$ for varying system parameters

D. *Robustness and stability margins*

The Bode diagram of the loop gain transfer function (18) with varying system parameters (J_s, b_s, K_s, R_s, m, J_m, R_m, b_m and b) is shown in Fig. 7. The stability margins of the system with the variant system parameters are shown in Table I.

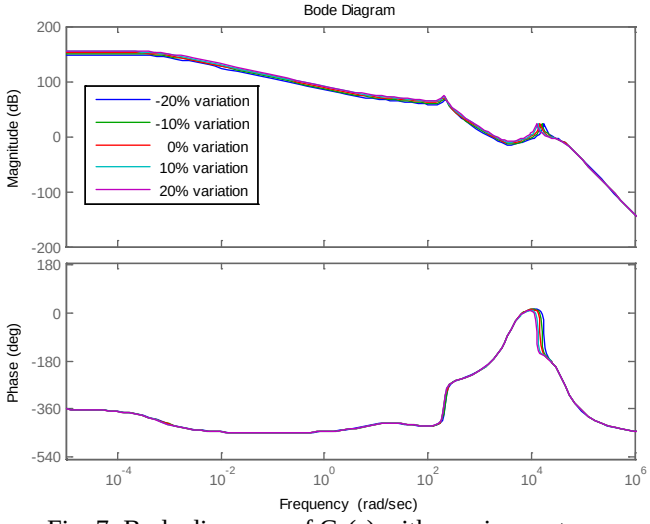

Fig. 7: Bode diagrams of $G_o(s)$ with varying system parameters

TABLE I: STABILITY MARGINS WITH DIFFERENT SYSTEM PARAMETERS

Changes in parameters	Gain margin(dB)	Phase Margin(deg)
-20%	8.98	7.13
-10%	8.63	7.14
0 %	10.77	10.16
10%	8.18	7.52
20%	8.69	7.07

From Fig. 7, we can see that as the system parameters are changing from -20% to 20% of their nominal values, the Bode diagrams are almost unchanged. Table I shows positive stability margins of the ADRC controlled EPAS system. The figure and table demonstrate the stability of the system in the presence of system uncertainties. The stability of the ADRC for a general n-th order physical plant is theoretically proved in [18]. The frequency-domain analyses introduced in this section confirmed the stability and robustness of the ADRC for this specific EPAS system.

E. Frequency responses with varying loop gain

The assist gain K_a in Fig.3 determines the driving and parking modes of a vehicle. As *Ka*=40, it represents parking mode where a large assistance for steering wheel is required. As *Ka*=1, it represents high-speed driving mode under which the assistant torque is much smaller than the one for parking mode. As *Ka* is ranging from 1 through 40, the driving speed is decreasing with the increase of *Ka*. The Bode diagrams of loop gain transfer function with varying assist gain *Ka* are given in Fig. 8.

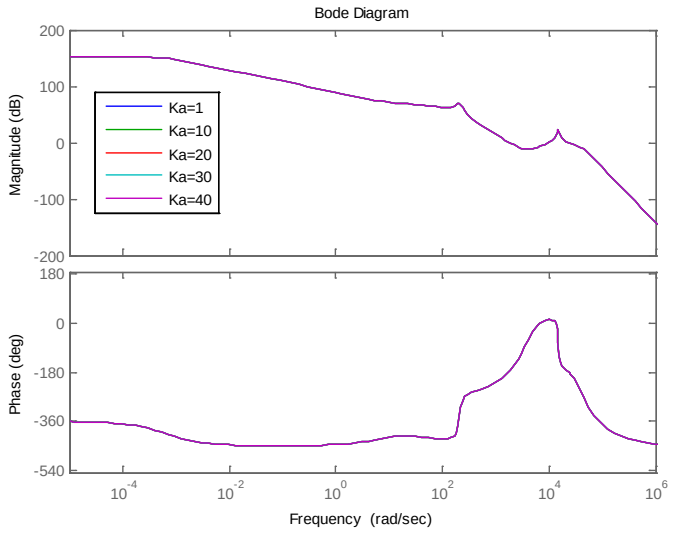

Fig.8: Bode plots of loop gain transfer function with changing assist gain (*Ka*)

Fig. 8 shows that the control system is robust against the variations of assist gain which represents different driving conditions with different speeds.

V. SIMULATION RESULTS

In order to verify the effectiveness of the ADRC, we apply it to the EPAS system shown in Fig. 3. The objective of the ADRC is to control the assist motor to generate a proper amount of assist torque so that the output steering torque T_s (measured by torque sensor) tracks a reference steering torque T_{rs}. As introduced in [8], the reference steering torque T_{rs} can be determined by a torque map based on the driving conditions (vehicle speed and steering wheel angle). In our simulation, we take T_{rs} as a step input signal with magnitude of *5Nm*, and the square-wave and sinusoidal signals with the amplitudes of *5Nm* and frequencies of *0.25Hz* respectively.

The simulation results are shown in Figs 9, 10, and 11, from which we can see that under the control of ADRC, the steering torques follows the reference steering torques very well. As a disturbance force (with the magnitude of 2*Nm*) is added to the EPAS system and the values of the parameters such as effective rack mass, damping and moment of inertia of the steering column are varying within 20% of the original values, the steering torque output still tracks the reference steering torque as well as the ones shown in Figs 8 through 10. Fig. 11 shows the external disturbance added to the system. Fig. 12 shows the ESO-estimated torque output approximates the real torque output very well in the presence of the disturbance.

The simulation results have validated the good tracking performance and the robustness of the ADRC against the disturbances and parameter variations successfully.

VI. CONCLUDING REMARKS

The technological advance in EPAS systems and their applications to the automobiles invariably bring on challenging control problems such as disturbance rejection, stabilization, and active compensation for modeling uncertainties. Furthermore, the space limitation of the EPAS system needs the control electronics to be as simple as possible. Therefore, multiple tuning parameters and complicated controller structure should be avoided. In this paper, an emerging practical controller ADRC is developed on a column-type EPAS system to reduce the torque efforts and to improve the steering feel of a driver. Both simulation results and frequency-domain analyses demonstrate the stability, robustness, and excellent tracking performance of the ADRC controller. In addition, the ADRC only has one tuning parameter, making it very simple to implement and to tune in the real world. We can conclude that the proposed research has successfully addressed the above problems of the EPAS system based on advanced control design techniques.

In the future, we plan to validate the EPAS controller design with lab and road testing. We also expect to enhance the range of the applications of the ADRC to other subsystems of the automobile, such as cruise control, anti-sliding control, and intelligent rollover detection and so on.

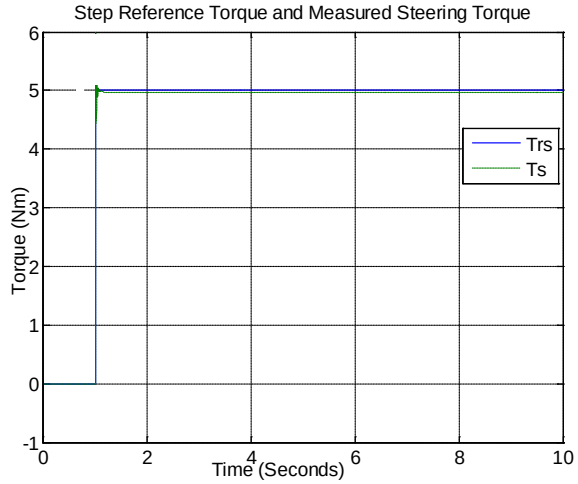

Fig.8: The step reference torque T_r and measured steering torque T_s without disturbance

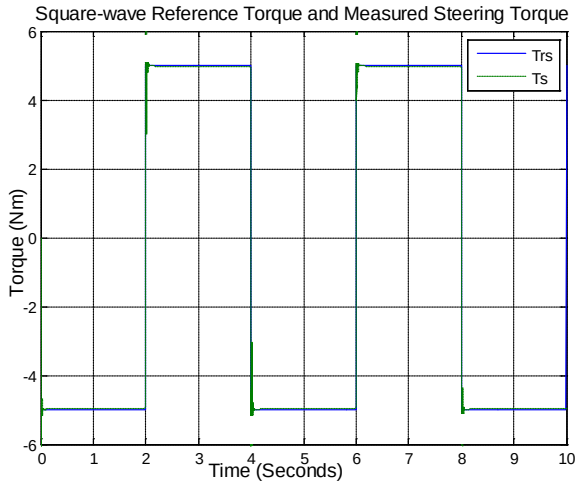

Fig.9: The square-wave reference torque and measured steering torque without disturbance

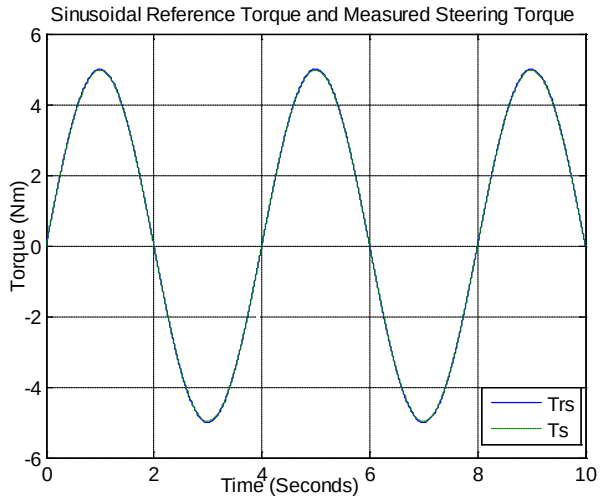

Fig.10: The sinusoidal reference torque and measured steering torque without disturbance

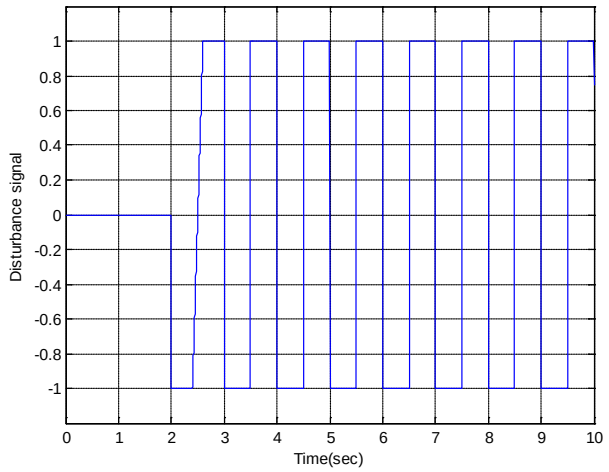

Fig. 11: Disturbance force

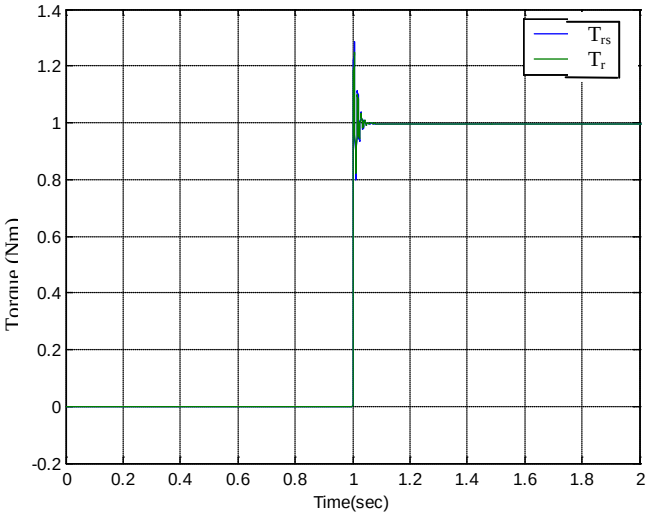

Fig. 12: The measured steering torque T_s with disturbance

APPENDIX

TABLE II: PARAMETER VALUES FOR AN EPAS SYSTEM

Pt=90π	Pa=200π	K_s=115	R_s=0.00778
b_s=0.36	G=7.225	m=32.1	J_m=0.0004707
b= 1365	b_m=0.00668	K_T=80000	m_e=438.04
J_s=0.04	R_m=0.00778	b_e=7413.98	K_e=1980000

$$A_d(s) = \beta b_6 s^{10} + (\beta b_5 + \beta b_6 \lambda_1)s^9 + (\beta b_4 + \beta b_6 \lambda_2)s^8 + (\beta b_3 + \beta b_4 \lambda_1 + \beta b_5 \lambda_2 + \beta b_6 \lambda_3)s^7 + (\beta b_2 + \beta b_3 \lambda_1 + \beta b_4 \lambda_2 + \beta b_5 \lambda_3 + \beta b_6 \lambda_4)s^6 + (\beta b_1 + \beta b_2 \lambda_1 + \beta b_3 \lambda_2 + \beta b_4 \lambda_3 + \beta b_5 \lambda_4 + \mu_1 a_2)s^5 + (\beta b_0 + \beta b_1 \lambda_1 + \beta b_2 \lambda_2 + \beta b_3 \lambda_3 + \beta b_4 \lambda_4 + \mu_2 a_2 + a_1 \mu_1)s^4 + (\beta \lambda_1 b_0 + \beta b_1 \lambda_2 + \beta b_2 \lambda_3 + \beta b_3 \lambda_4 + \mu_3 a_2 + a_1 \mu_2)s^3 + (\beta b_0 \lambda_2 + \beta b_1 \lambda_3 + \beta b_2 \lambda_4 + \mu_4 a_2 + a_1 \mu_3)s^2 + (\beta b_0 \lambda_3 + \beta b_1 \lambda_4 + \mu_5 a_2 + a_1 \mu_4)s + \beta \lambda_4 b_0 + a_1 \mu_5$$

REFERENCES

[1] J. Kim, J. Song, "Control Logic for an Electric Power Steering System Using Assist Motor", *Mechatronics*, vol. 12, no. 3, pp. 447-459, Apr. 2002.

[2] G. L. Nikulin and G. A. Frantsuzova, "Synthesis of an Electric-power Steering Control System", *Optoelectronics, Instrumentation and Data Processing*, vol. 44, no. 5, pp. 454-458, 2008.

[3] H. Akhondi, J. Milimonfared, "Performance Evaluation of Electric Power Steering with IPM Motor and Drive System", in *Proc. of IEEE Region 8 International Conference on Computational Technologies in Electrical and Electronics Engineering*, Novosibirsk, Russia, Jul. 2008, pp. 175-179.

[4] J. Song, K. Boo, H. S. Kim, J. Lee, and S. Hong, "Model Development and Control Methodology of a New Electric Power Steering System", in *Proc. of Institution of Mechanical Engineers, Part D: J. Automobile Engineering*, vol. 218, 2004, pp.967-975.

[5] Y. Morita, K. Torii, N. Tsuchida, et al.., "Improvement of Steering Feel of Electric Power Steering System with Variable Gear Transmission System Using Decoupling Control", in *Proc. of 10th IEEE International Workshop on Advanced Motion Contro*l, Trento, Italy, Mar. 2008, pp.417-422.

[6] H. Zang, M. Liu, "Fuzzy Neural Network PID Control for Electric Power Steering System", in *Proc. of IEEE International Conference on Automation and Logistics*, Aug. 2007, pp. 643-648.

[7] J. Lee, H. Lee, J. Kim, and J. Jeong, "Model-based Fault Detection and Isolation for Electric Power Steering System", in *Proc. of International Conference on Control, Automation, and System*, Oct. 2007, pp. 2369-2374.

[8] A.T. Zaremba, M.K. Liubakka, R.M. Stuntz, "Vibration Control Based on Dynamic Compensation in an Electric Power Steering System", in *Proc. of the first international conference on Control of Oscillations and Chaos*, San Petersburg, Russia, Aug. 1997, vol. 3, pp. 453-456.

[9] A. T. Zaremba, M. K. Liubakka, R. M. Stuntz, "Control and Steering Feel Issues in the Design of an Electric Power Steering System", in *Proc. of the American Control Conference*, Philadelphia, PA, Jun. 1998, pp. 36-40.

[10] R. C. Chabaan, L. Y. Wang, "Control of Electrical Power Assist Systems: H^{∞} Design, Torque Estimation and Structural Stability", *JSAE Review 22*, pp. 435-444, 2001.

[11] Z. Gao, "Active Disturbance Rejection Control: A Paradigm Shift in Feedback Control System Design," in *Proc. of American Control Conference*, Minneapolis, MN, June 2006, pp.2399-2405.

[12] Z.Gao, Y. Huang, and J. Han, "An alternative paradigm for control system design," in *Proc. of IEEE conference on Decision and Control*, Orlando, Florida, Dec. 2001, vol. 5, pp. 4578–4585.

[13] Z.Gao "Scaling and Parameterization Based Controller Tuning," in *Proc. of the 2003 American Control Conference*, Denver, CO, Jun. 2003, vol. 6, pp. 4989–4996.

[14] L. Dong, D. Avanesian, "Drive-Mode Control for Vibrational MEMS Gyroscopes," *IEEE Transaction on Industrial Electronics*, vol. 56, no. 4, pp. 956–963, 2009.

[15] L. Dong, Q. Zheng, and Z. Gao, "On Control System Design for the Conventional Mode of Operation of Vibrational Gyroscopes", *IEEE Sensors Journal*, vol. 8, no. 11, pp. 1871-1878, Nov. 2008.

[16] G. Tian, and Z. Gao, "Frequency Response Analysis of Active Disturbance Rejection Based Control System," in *Proc. of IEEE International Conference on Control Applications*, Singapore, Oct. 2007, pp. 1595–1599.

[17] Z. Gao, "Scaling and bandwidth-parameterization based controller tuning," in *Proc. of American Control Conference*, Denver, CO, June 2003, vol. 6, pp. 4989-4996.

[18] Q. Zheng**,** L. Dong, D. H. LEE, Z. Gao, "Active Disturbance Rejection Control for MEMS Gyroscopes", *IEEE Transaction on Control Systems and Technology*, vol. 17, no. 6, pp. 1432-1438, Apr. 2009.